9th Asia-Pacific Conference on Wind Engineering

Auckland, New Zealand

3-7 December 2017

Effects of Turbulence and Nonuniformly Distributed Mean Wind on Vortex-induced Vibration of a Long-span Bridge

Q. Zhu[1,3], Y.L. Xu[2] and L.D. Zhu[1,3,4]

[1]Department of Bridge Engineering, Tongji University, Shanghai 200092, China

[2]Department of Civil and Environmental Engineering,

The Hong Kong Polytechnic University, Hong Kong, China

[3]State Key Laboratory of Disaster Reduction in Civil Engineering, Tongji University, China

[4]Key Laboratory of Wind Resistance Technology of Bridges of Transport Ministry,

Tongji University, Shanghai 200092, China

Abstract

With the increase of span length, long-span bridges are more flexible and therefore more susceptible to vortex-induced vibrations (VIV). Accurate predictions of the structural responses caused by VIV are important as sometimes a certain degree of VIV is inevitable. Turbulence and the nonuniformly distributed wind speed are highly likely to affect the VIV responses but were never considered in the existing VIV analysis methods. A VIV analysis method is developed in this paper to involve the effects of turbulence, as well as the nonuniformly distributed mean wind speed along the bridge axis. The developed method is applied on a long-span suspension bridge with a twin-box deck that suffers VIV. The analytical results are compared with the on-site VIV responses recorded by the monitoring system on that bridge. Results show that both the turbulence and the nonuniform distribution of mean wind speed can notably reduce the VIV responses.

Introduction

Vortex-induced vibration (VIV) is a typical vibration caused by the interaction of a bridge and the incoming wind. Although VIV does not directly cause a bridge to collapse, it may cause fatigue damage in crucial components of the bridge and impair the driving safety of vehicles. Many long-span cable-supported bridges have suffered VIV, including the Second Severn Crossing in the UK [10], the Deer Isle Bridge in the US [5], the Great Belt Bridge in Denmark [6], and the Xihoumen Bridge in China [8].

With the increase of span length, long-span bridges are more flexible and therefore more susceptible to VIV. In practice, sometimes VIV with small amplitudes can be allowed on long-span bridges as long as the safety and serviceability of the structure are ensured. This highlights the importance of accurate predictions of the structural responses caused by VIV.

The prediction methods of such responses are usually based on the wind tunnel tests on aeroelastic section models of bridge decks. These methods generally fall into two categories.

The first category directly uses the results of tests on section models to predict the responses of the prototype bridge. Ehsan and Scanlan [3] used Scanlan's semi-empirical model for vortex-induced force (VIF) to solve the motion equation for the whole bridge with the test-identified parameters. Irwin [4] directly deduced the relationship between the maximum displacement of the test model and that of the prototype bridge. These methods are simple and effective linear estimations of the VIV responses of the prototype bridges. Neither the non-linearity in the VIF nor that in the structural behavior can be considered in these methods. Furthermore, the vortex-induced internal forces on the bridge, which are important for fatigue analyses, cannot be directly obtained by these methods.

The second category uses semi-empirical models for VIF to obtain VIF time-histories from section model tests, and then apply the identified VIFs on models of the bridges for responses. Barhoush et al. [1] used the Newmark-Beta method to obtain the solution for the VIV of finite-element frame models with a two-degree-of-freedom semi-empirical VIF model. Diana et al. [2] solved the VIV on a finite-element bridge deck model with equivalent oscillators using the two-degree-of-freedom semi-empirical VIF model proposed in the same paper. Considering the fact that the VIV of a bridge are always excited one mode at a time, Meng et al. [11] has proposed a mode-by-mode solution method for VIV of the prototype bridge based on a nonlinear single-degree-of-freedom VIF model proposed by the same group [12].

All the above mentioned VIV analysis methods only takes account of a uniform incoming wind. Neither the turbulence nor the nonuniform distribution of wind speed along the bridge axis can be involved in these analyses. However, a certain level of turbulence always exists on bridge site; and for long-span bridges, the incoming wind is not uniformly distributed along the bridge axis. These two factors are very likely to affect the VIV responses and need to be investigated in order to achieve an accurate prediction of VIV for long-span bridges.

This paper aims to develop the mode-by-mode VIV analysis method proposed by Meng et al. [11] to involve the effects of the turbulence and nonuniform distribution of mean wind speed. A VIF model proposed by Zhu et al. [14] for vortex-induced vertical forces on twin-box decks under turbulent wind flow is used. The whole-bridge VIV analyses results are then compared with the site-measured data of a long-span suspension bridge with a twin-box deck.

Wind tunnel tests for VIF under turbulence

Wind tunnel tests on the section model of the Xihoumen Bridge deck were carried out in the TJ-3 boundary layer wind tunnel of

the State Key Laboratory for Disaster Reduction in Civil Engineering at Tongji University, China (see Figure 1). The twin-box deck of the Xihoumen Bridge is simulated using a section model with a scale ratio of 1:20. The model is 3.6 m in length, 1.8 m in width (with a 0.3 m slot between the boxes) and 0.175 m in depth.

A newly-developed wind tunnel testing technique was used to obtain the VIF time-histories on the elastically-mounted twin-box section model [12,13]. 7 pairs of force-measuring strips were embedded in the model (see Figure 2). Each strip was made of light polymeric foam and some auxiliary parts that allow the polymeric foam to be connected to the inner rigid frame through a force balance. Force balances were installed to directly connect the force measurement strips to the inner rigid frame. Marginal gaps of 1mm width between the polymeric foam strip and the wooden-plate skinned rest of the model were retained so that the forces recorded by the force balances are only the inertia and aerodynamic forces acting on the light foam strip, each of which weighs only about 0.094 kg. The use of narrow force-measuring strips can largely reduce the proportion of inertia forces in the measured data and therefore improve the accuracy of acquired VIFs. By subtracting the inertial and non-wind-induced force from the recorded force time-histories, the time-histories of the VIF can be acquired [13]. The parameters described in the semi-empirical VIF model can then be identified from these VIF time-histories.

Tests under both smooth flow and turbulent flow were conducted. The turbulent flow fields were generated by grids consisting of vertical and horizontal aluminium alloy strips. The time-histories of the VIF acquired form these tests were investigated to propose the VIF model considering turbulence effects. The VIV observed under both smooth and turbulent flow with different structural damping were used to validate the proposed VIF model.

Figure 1. Mounted section model in the wind tunnel

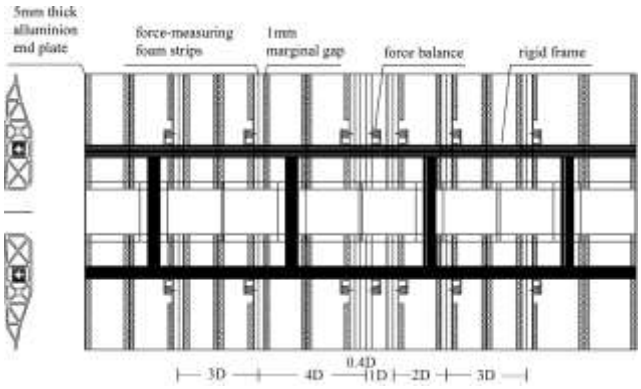

Figure 2. Plan layout of the section model

Semi-empirical VIF model for twin-box decks under turbulent wind flow

The motion equation of a two-dimensional bridge deck section under vertical VIF can be written as

$$\ddot{\eta}(s) + 2\zeta K_1 \dot{\eta}(s) + K_1^2 \eta(s) = \tilde{F}_{VI} \qquad (1)$$

where $\eta=y/D$ is the dimensionless vertical displacement; D is the deck depth; $K_1=\omega_1 D/U$ is the reduced natural frequency; U is the wind speed perpendicular to the bridge deck; $s=Ut/D$ is the dimensionless time; the over-dot here denotes differentiation with respect to the dimensionless time; and $\tilde{F}_{VI}$ is the dimensionless VIF.

A two-dimensional VIF model for a twin-box deck considering the turbulence effects have been proposed by Zhu et al. [14] based on the results observed in the wind-tunnel tests introduced in the last section. The VIF model can be expressed as

$$\tilde{F}_{VI} = m_r \left[Y_1(K) \cdot \left(1-\varepsilon(K)\dot{\eta}^2-\varepsilon_t w_r^2\right) \cdot \dot{\eta} + Y_2(K)\eta \right] \qquad (2)$$

where $Y_1(K)$, $Y_2(K)$, and $\varepsilon(K)$ are the parameters to be determined by wind tunnel tests under smooth incoming wind flow; K is the reduced frequency; ε_t is the to-be-determined parameter regarding the turbulence effects; $m_r=m/\rho D^2$ is the structural mass ratio in which ρ is the air density; w_r is the non-dimensional vertical turbulent wind speed as $w_r=w/U$ where w is the vertical turbulent wind speed and U is the mean wind speed.

The proposed VIF model includes all the non-conservative motion-induced force terms. The validity of the proposed VIF model was examined by wind tunnel tests described in the last section. The results show that this model can effectively predict the maximum vortex-induced response of a twin-box bridge deck under different turbulent fields. The prediction accuracy for cases with different structural damping ratio/Scruton number are also acceptable [14]. The parameters in the VIF model for the Xihoumen Bridge deck were identified with the VIF time-histories extracted from those acquired total force time-histories and are listed in table 1. The the reduced wind speed is calculated as U/fD, where f is the vertical frequency of the model.

Reduced wind speed	Y_1	Y_2	ε	ε_t
6.026	1.63	3.998	85.7	115.1
6.390	9.95	4.801	161	115.1
6.733	35.10	4.645	285.2	115.1
7.077	50.02	4.726	351.7	115.1
7.428	48.50	4.983	422.6	115.1
7.778	41.10	5.445	593.4	115.1
8.135	30.65	5.883	949.8	115.1
8.493	18.24	6.52	1671	115.1
8.823	1.74	7.104	8464.3	115.1
9.187	12.50	8.726	4817	115.1

Table 1. Identified parameters of the VIF on the Xihoumen Bridge deck.

Whole-bridge VIV analysis on a long-span bridge considering turbulence and nonuniform mean wind

With the proposed VIF model, the motion equation of the VIV can be written as

$$\begin{aligned} &\ddot{\eta}(s) + 2\zeta K_1 \dot{\eta}(s) + K_1^2 \eta(s) \\ &= m_r \left[Y_1(K) \cdot \left(1-\varepsilon(K)\dot{\eta}^2-\varepsilon_t w_r^2\right) \cdot \dot{\eta} + Y_2(K)\eta \right] \end{aligned} \qquad (3)$$

For the lower-order natural frequencies around which lock-in vibrations usually occur, it can be assumed that these frequencies are well separated and lock-in vibrations only occur at a single mode each time. In such cases, the non-dimensional vertical displacement η at the span-wise location x of the deck can be expressed as

$$\eta(x,s) = \Phi(x)v(s) \qquad (4)$$

where $\Phi(x)$ is the non-dimensional mode shape for the VIV; $v(s)$ is the generalized coordinate.

Multiply $\Phi(x)$ on both sides of Eq.(3), and then conduct integration along the bridge axis; the generalized governing equation considering the nonuniform distribution of mean wind speed as

well as turbulence along the bridge axis can be written as follows noting that in the cases that the wind speed varies span-wisely, the parameters Y_1, Y_2 and ε are functions of x as they are functions of the mean wind speed.

$$\begin{aligned}&\int_0^L m_r\Phi^2(x)\mathrm{d}x\cdot\left[\ddot{v}(s)+2\zeta K_1\dot{v}(s)+K_1^2v(s)\right]\\&=\rho D^2\Big[\dot{v}(s)\int_0^L Y_1(K)\Phi^2(x)dx-\dot{v}^3(s)\int_0^L Y_1(K)\varepsilon(K)\Phi^4(x)dx\\&-\varepsilon_i\dot{v}(s)w_r^2(s)\int_0^L Y_1(K)\Phi^2(x)dx+v(s)\int_0^L Y_2(K)\Phi^2(x)dx\ \Big]\end{aligned}\tag{5}$$

where L is the total length of the bridge deck.

When the mode shapes are mass-normalized as

$$\int_0^L m\Phi^2(x)\mathrm{d}x=1\tag{6}$$

Eq.(5) can be rewritten as

$$\begin{aligned}&\ddot{v}(s)+2\zeta K_1\dot{v}(s)+K_1^2v(s)\\&=\rho D^2\Big[\dot{v}(s)\int_0^L Y_1(K)\Phi^2(x)dx-\dot{v}^3(s)\int_0^L Y_1(K)\varepsilon(K)\Phi^4(x)dx\\&-\varepsilon_i\dot{v}(s)w_r^2(s)\int_0^L Y_1(K)\Phi^2(x)dx+v(s)\int_0^L Y_2(K)\Phi^2(x)dx\ \Big]\end{aligned}\tag{7}$$

If not considering the turbulence and the nonuniformity of the incoming wind, Eq.(7) can be reduced to

$$\begin{aligned}&\left[\ddot{v}(s)+2\zeta K_1\dot{v}(s)+K_1^2v(s)\right]=\rho D^2\Big[Y_1(K)\dot{v}(s)\int_0^L\Phi^2(x)\mathrm{d}x\\&-\varepsilon(K)Y_1(K)\dot{v}^3(s)\int_0^L\Phi^4(x)\mathrm{d}x+Y_2(K)v(s)\int_0^L\Phi^2(x)\mathrm{d}x\ \Big]\end{aligned}\tag{8}$$

Both Eq.(7) and Eq.(8) can be solved mode-by-mode with Newmark-Beta method for VIV responses.

Xihoumen Bridge and its recorded VIV events

The Xihoumen Bridge is a suspension bridge located on the east coast of China with a main span of 1650 m and a side span of 578 m. The super-long-span bridge suffers strong typhoons and monsoons with high wind speed. As a result, a twin-box deck was adopted for its exceptional performance against flutter. However, the geometry of the deck makes the bridge especially susceptible to VIV at low wind speeds.

A comprehensive structural health monitoring system has been installed on the bridge to monitor its performance and safety. Monitoring the wind and wind effects on the bridge is a major objective of this system. A detailed introduction to the sensors regarding this objective can be found in the works of Li et al. [8,9]. Some important information of the sensors regarding the work in this paper is presented as follows. Six anemometers have been installed at the middle and quarter points of the central span. The anemometers are installed 6 m above the deck surface. Three sets of accelerometers are also installed at the middle and quarter points of the central span to record he lateral and vertical accelerations of the deck.

Thirty-seven observed VIV events have been reported in the work of Li et al. [9]. Seven of these events occurred with the 8th mode of the bridge, which is also the 6th vertical bending mode with a frequency of 0.183 Hz and a structural damping ratio of 0.5%. Twenty-three of these events occurred with the 22nd mode of the bridge, which is also the 10th vertical bending mode with a frequency of 0.327 Hz and a structural damping ratio of 0.42%. The on-site data of the 22nd mode are used in this paper for comparison with analytical results. The mode shape of the 22nd mode is plotted in Figure 3.

Some of the observed VIV events on the 22nd mode with large VIV responses are listed in table 2. Event 17 is the largest VIV recorded on this mode. The mean wind speed recorded by the south anemometer and that by the north anemometer are notably different. Such nonuniform distributions of mean wind along the bridge axis are normal considering the long span length of the bridge. The effects of this on the VIV, however, have never been studied. The turbulence intensity level of the observed events is about 5%.

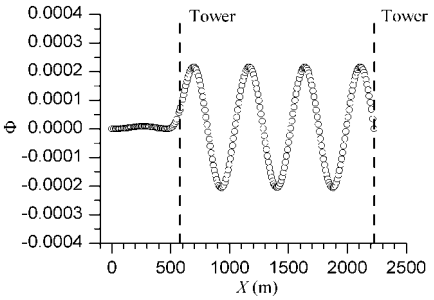

Figure 3 Mode shape of the 22nd mode of the Xihoumen Bridge

Events	U_{South} (m/s)	U_{North} (m/s)	U_{Mean} (m/s)	$I_{u,Mean}$ (%)	Max Displacement (m)
E8	11.2	12.71	11.955	5.15	11.89
E9	9.73	10.68	10.205	4.555	9.61
E11	9.75	10.44	10.095	5.985	4.64
E16	10.44	11.33	10.885	5.145	14.78
E17	10.2	12	11.1	4.755	17.1

Table 2. Characteristics of some recorded VIV events

Results and Discussions

With the VIF model and the identified parameters listed in table 1, the motion equation of the VIV on the mode 22nd of the Xihoumen Bridge can be solved by Newmark-Beta method.

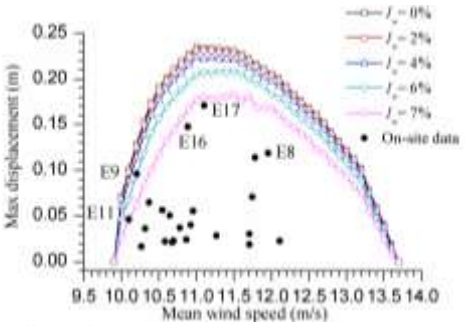

Figure 4. Effects of turbulence on the VIV response and comparison between analytical and field-measurement responses

Figure 4 shows the effects of the turbulence on the maximum displacement responses in the analytical results as well as the field-measurement maximum displacements. The analytical responses were computed with the uniformly distributed mean wind speed, which was taken as the mean value of the north and south records. The turbulence does not affect the lock-in range of VIV but can obviously reduce the maximum displacement responses. Judging from the analytical results, an 8% vertical turbulence intensity reduces the maximum displacement by about 30%. On the 22nd mode, the VIV events E11, E9, E16, E17 and E8 generally represents the site-measured maximum displacement curve of the lock-in range. But the maximum displacement of most other events falls far below this curve, indicating the VIV in these events

are not fully developed. The analytical VIV responses are remarkably larger than the field-measured responses. The largest analytical maximum displacement is about 50% larger than the largest field-measured value, which is the responses recorded in Event 17.

Figure 5 shows the analytical VIV time-histories of event E17 in three cases. The first case takes account of neither the turbulence nor the nonuniform mean wind speed. The second case was computed with the nonuniform mean wind speed without turbulence. The third case considers both nonuniformities. The results show that, first, both the nonuniform distribution of mean wind speed and the turbulence can effectively reduce the maximum VIV displacement; second, turbulence not only reduces the maximum displacement but also introduce fluctuation in the vibration amplitude; third, the analytical maximum displacement considering the turbulence and the nonuniform distribution of mean wind speed is very close to the site-measured value.

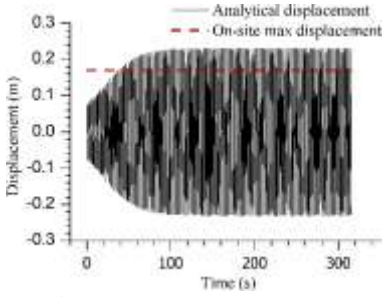

(a) uniform mean wind speed + no turbulence

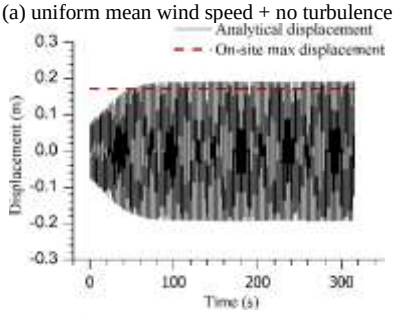

(b) nonuniform mean wind speed + no turbulence

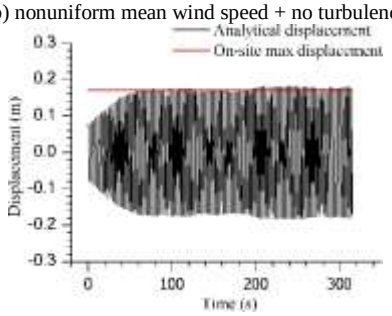

(c) nonuniform mean wind speed + turbulence

Figure 5 Analytical VIV time-histories of event E17 in different cases

Conclusions

A VIV analysis method is developed to involve the effects of turbulence, as well as the nonuniformly distributed mean wind speed along the bridge axis. The developed method is applied on a long-span suspension bridge with a twin-box deck that suffers VIV. The analytical results are compared with the on-site VIV events recorded by the monitoring system.

Results show that both the turbulence and the nonuniform distribution of mean wind speed reduce the VIV responses. For long-span bridges, neglecting the nonuniform distribution of wind speed may overestimate the VIV responses.

Acknowledgments

The authors wish to acknowledge the financial support from the National Natural Science Foundation of China (Grants 51478360, 91215302, 51323013 and 51608389), and that from the Research Grants Council of Hong Kong (PolyU5285/13E).

References

[1] Barhoush, H., Namini, A.H. and Skop, R.A., Vortex shedding analysis by finite elements, *J. Sound Vib.*, **184**(1), 1995, 111-127.

[2] Diana, G., Resta, F., Belloli, M. and Rocchi, D., On the vortex shedding forcing on suspension bridge deck, *J. Wind Eng. Ind. Aerodyn.*, **94**(5), 2006, 341-363.

[3] Ehsan, F. and Scanlan, R.H., Vortex-induced vibrations of flexible bridges. *J. Eng. Mech.*, **116**(6), 1990, 1392-1411.

[4] Irwin, P.A., The role of wind tunnel modelling in the prediction of wind effects on bridges, in *Proceedings of the International Symposium Advances in Bridge Aerodynamics*, Copenhagen, Balkema, Rotterdam, 1998, 99–117.

[5] Kumarasena, T., Scanlan, R.H. and Ehsan, F., Wind-induced motions of Deer Isle bridge, *J. Struct. Eng.*, **117**(11), 1991, 3356-3374.

[6] Larsen, A., Esdahl, S., Andersen, J.E. and Vejrum, T., Storebælt suspension bridge–vortex shedding excitation and mitigation by guide vanes. *J. Wind Eng. Ind. Aerodyn.*, **88**(2), 2000, 283-296.

[7] Lewandowski, R., Non-linear steady state vibrations of beams excited by vortex shedding. *J. Sound Vib.*, **252**(4), 2002, 675-696.

[8] Li, H., Laima, S., Ou, J., Zhao, X., Zhou, W., Yu, Y., ... and Liu, Z., Investigation of vortex-induced vibration of a suspension bridge with two separated steel box girders based on field measurements. *Eng. Struct.*, **33**(6), 2011, 1894-1907.

[9] Li, H., Laima, S., Zhang, Q., Li, N. and Liu, Z., Field monitoring and validation of vortex-induced vibrations of a long-span suspension bridge. *J. Wind Eng. Ind. Aerodyn.*, **124**(7), 2014, 54-67.

[10] Macdonald, J.H., Irwin, P.A. and Fletcher, M.S., Vortex-induced vibrations of the Second Severn Crossing cable-stayed bridge—full-scale and wind tunnel measurements, *Proceedings of the Institution of Civil Engineers—Structures and Buildings*, **152**(2), 2002, 123-134.

[11] Meng, X.L., Zhu, L.D., Xu, Y.L. and Guo, Z.S., Imperfect correlation of vortex-induced fluctuating pressures and vertical forces on a typical flat closed box deck. *Adv. Struct. Eng.*, **18**(10), 2015, 1597-1618.

[12] Zhu, L.D., Meng, X. L. and Guo, Z.S., Nonlinear mathematical model of vortex-induced vertical force on a flat closed-box bridge deck, *J. Wind Eng. Ind. Aerodyn.*, **122**, 2013, 69-82.

[13] Zhu, Q., Chen, B.Y., Zhu, L.D. and Xu, Y.L., Investigation on characteristics and span-wise correlation of vortex-induced forces on a twin-box deck using newly-developed wind-tunnel test technique, *J. Wind Eng. Ind. Aerodyn.*, **164**, 2017, 69-81.

[14] Zhu, Q., Xu, Y.L., Zhu, L.D. and Chen, B.Y., A semi-empirical model for vortex-induced vertical forces on a twin-box deck under turbulent wind flow, *J. Fluids Struct.*, **71**, 2017, 183-198.